Active damping using Smart Discs

For the development of precision machinery, a limited number of well-known design principles apply. They include stiffness management, 'weight watching', kinematic design, and elimination of friction and backlash. A disadvantage of constructions designed in this way is a lack of damping. The Smart Disc concept uses piezoelectric sensors and actuators to actively dampen vibrations. The challenge in designing accurate, well-dampened machine frames lies in having the control technology – in itself not overly complicated – accepted as an established design principle.

This article is a compilation of two articles that were previously published (in Dutch) in Mikroniek, 2002, no. 5 and 2005, no. 4.

• *Jan Holterman and Theo J.A. de Vries* •

Large spacecrafts must be extremely light, and consequently, usually are very flexible and easily induced to vibrate. Damping the vibrations is no simple task. Traditional, passive solutions such as applying visco-elastic materials to large surfaces quickly add too much weight to the equation. In space travel, therefore, it seemed obvious to switch to active damping with sensors that can measure the vibrations and actuators that can reduce them.

In precision machinery, active vibration control in the form of vibration isolation is not new either. Most disturbances enter through the floor, which is a reason to place the machinery on special vibration isolators. If necessary, the combination of a passive system and an actively controlled system offers a solution. The passive system then ensures isolation of high-frequency disturbances and the active system ensures the correct static position of the machinery and sufficient damping of the low-frequency suspension modes. A machine frame has many more vibration modes, which mainly describe internal deformations of the frame at higher frequencies. To minimise their negative influence on accuracy, the frame must, to begin with, be as stiff as possible and have a mass as small as possible (the principles of 'stiffness management' and 'weight watching'). However, stiffness cannot be increased limitlessly. The designer also has to take into account other design principles such as 'kinematic design' [4].

Wafer scanner lens suspension

Take the suspension of a wafer scanner lens (see the box). In Figure 1, the so-called main plate represents the 'clean world'. It stands on three air mounts (active pneumatic vibration isolators) and is almost unaffected by vibrations from the floor. The lens is suspended in a circular hole made in the main plate. This lens is, in fact, a stack of lenses with a total height of about 1 m and a diameter of 0.5 m. The lens is set in a flange that, in turn, is mounted to the main plate with the aid of three identical steel blocks, the so-called lens supports.

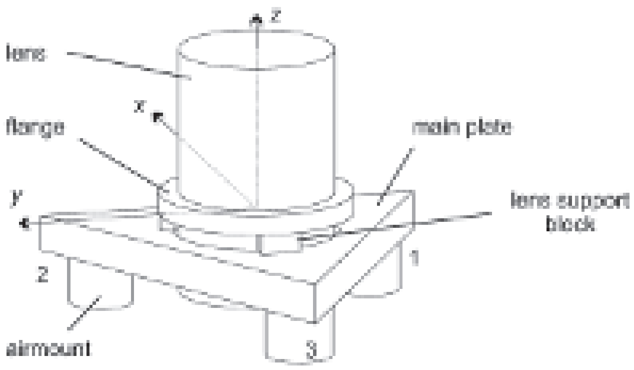

Figure 1. Diagram of the lens suspension in a wafer scanner.

In order to define all six degrees of freedom of the lens exactly once (the principle of 'kinematic design'), each of the lens supports must define two coordinates, vertical and tangential (y and z in Figure 2). Locally, the remaining four coordinates must be left free and, for that, a lens support must be fitted with various hinges. In order to avoid backlash and friction, notorious sources of inaccuracy, the use of elastic hinges is an obvious choice [4].

A conventional lens support is fitted with two horizontal elastic hinges across the entire length (see Figure 2). This means, however, that for each suspension point only two coordinates (x en φ_x) are left free, whereas it should have been four coordinates. This is the result of a trade-off between the principles of 'stiffness management' and 'kinematic design': a lens support with more than two elastic hinges would result in too much stiffness loss.

Wafer scanner

Wafer scanners are used in the production of ICs (integrated circuits). Through a lithographic process, they apply a pattern of electronic circuits onto a silicon wafer. The reticle with the desired pattern is positioned by a stage at the top of the machine. The wafer is positioned by the wafer stage. Between both stages, there are various stacked lenses (in short, lens). This lens projects the desired pattern onto the silicon. The non-exposed material on the wafer is etched away, so that a circuit with the desired form remains. The smaller the pattern, the more circuits per wafer and the faster the chips.
The wafer scanner is an excellent example of a precision machine; the specifications are formulated in terms of nanometres. The lens suspension of a wafer scanner frame that was specially adapted for this purpose served as the test assembly for the Smart Disc experiments described here.

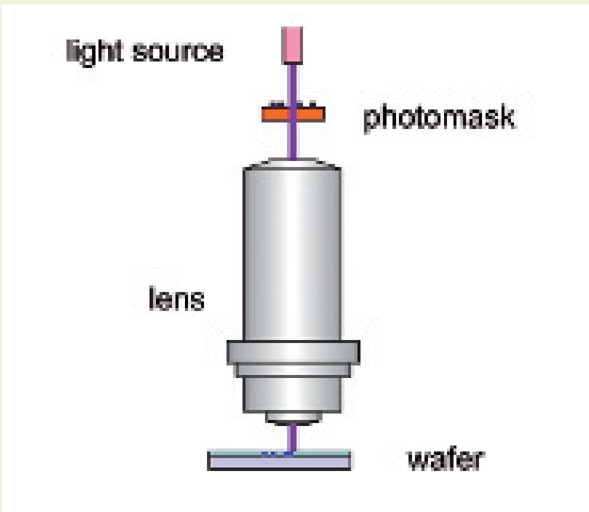

Figure A. Simple representation of the lithographic process in a wafer scanner.

A consequence is that the two end surfaces of a lens support, and with these the corresponding reference surfaces in the machine, must be presented sufficiently parallel.

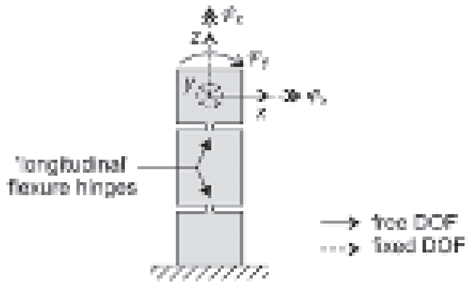

Figure 2. Diagram of a conventional lens support.

For the analysis of the system (main plate and lens, together properly isolated from the floor) we assume, for the sake of convenience, that no internal deformation occurs. The dynamic behaviour can then be characterised by six vibration modes of the lens with respect to the main plate (Figure 3):

- Two joystick modes, with the lowest natural frequencies (approx. 100 Hz). In these modes, the lens tilts around an axis in the suspension plane (x-y-surface in Figure 1). These modes are due to the limited vertical stiffness of the lens supports.
- Two pendulum modes. The lens moves more or less horizontally in the suspension plane. These modes are particularly due to the limited horizontal stiffness, i.e. the shear stiffness of the lens supports.
- In the two remaining vibration modes (not shown in Figure 3), there is relative vertical displacement and relative rotation around the vertical axis, respectively.

In the wafer scanner, the joystick modes and, to a lesser extent, the pendulum modes result in the highest vibration levels.

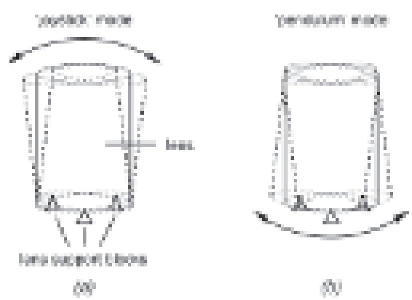

Figure 3. Diagram of the dominant vibration modes of the lens with respect to the main plate.

Reference experiment

This article firstly focuses on active damping of both joystick modes. To make a joystick mode clearly visible, a reference experiment was carried out [6]. For this experiment, it was attempted to measure the joystick rotation around the (randomly chosen) x-axis in Figure 1, or rotation in the drawing surface in Figure 4. The air mounts were used to introduce a controllable disturbance to the main plate, the torque T_{am} around the x-axis. This torque is a white noise signal (0-300 Hz). The spectrum of the disturbance is therefore flat in a sufficiently broad frequency range.

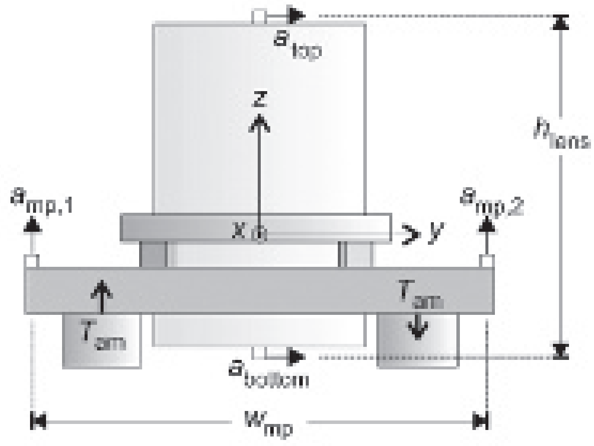

Figure 4. Side view of the test set-up for determining the joystick rotation around the *x*-axis.

The joystick rotation $\varphi_x(t)$ cannot be measured directly. Instead, the rotation is reconstructed from four acceleration measurements, on the lens and the main plate (the white squares in Figure 4), with the aid of the following equation:

$$\varphi_x(t) = \iint \left[\frac{a_{bottom}(t) - a_{top}(t)}{h_{lens}} - \frac{a_{mp,2}(t) - a_{mp,1}(t)}{w_{mp}} \right] (dt)^2$$

The results of the reference experiment are shown in Figure 5 (also see the box).

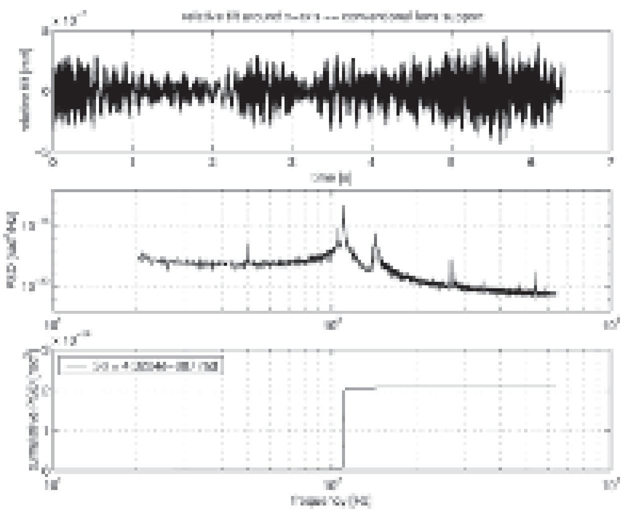

Figure 5. Results of the reference experiment.
Top: the reconstructed joystick rotation.
Middle: the accompanying Power Spectral Density *PSD*.
Bottom: the accompanying cumulative *PSD*.

This reference experiment shows an amplitude of the joystick rotation of 0.43 μrad. Furthermore, it appears from the steep step around 110 Hz in the cumulative *PSD* that this rotation emanates almost completely from the lack of damping of the joystick modes. Further inspection of the measuring results has revealed that the damping ratio of the joystick modes amounted to only 0.2% [6].
In theory, this low value of the damping does not have to be a problem but in practice it is impossible to isolate the lens and the main plate completely from all disturbing forces in the vicinity. The acoustics turn out to be the most important source of disturbance; the air in the system moves around a lot.

The obvious solution is to increase the damping in the system. Passive damping in mechanical systems, however, is mainly caused by friction and this is mostly disastrous for accuracy. Just as in space travel, the step to active damping is a logical one. The main challenge with this is to guarantee the stability of the controlled system. The control design is based on a model, i.e. a simplification of reality. Non-modelled vibration modes can easily cause instability. The simplest way to prevent this is to use the collocated control principle: the closing of a control loop between a sensor and an actuator that are positioned at the same place in the system [5].

Power Spectral Density

Two important characteristics of a signal *x(t)* are the mean μ and the standard deviation σ. The power *P* of a signal is equal to the sum of μ squared and σ squared. A suitable measure for the amplitude of a noisy signal is the 3σ value. A normally distributed signal is within the limits $[\mu-3\sigma, \mu+3\sigma]$ for 99.7% of the time. For the contribution of certain vibration modes to the amplitude of the measured signal, the frequency content of the signal is important. The Power Spectral Density, *PSD(f)*, is a measure of the power at frequency *f*. The cumulative *PSD* is defined as the surface under the *PSD* up to frequency *f*:

$$cumPSD(f) = \sum_0^f PSD(\rho)d\rho$$

The end value of *cumPSD* is equal to the total signal power. When μ is equal to zero, the standard deviation can be calculated from the end value of *cumPSD*:

$$\sigma = \sqrt{cumPSD(f_{max})}$$

and with this the 3σ value can then be determined.
The following is derived from Figure 5:

$$3\sigma = 3\sqrt{2.1 \cdot 10^{-14}} = 0.43\ \mu rad^{1/2}$$

The cumulative *PSD* in Figure 5 shows that this power is almost totally attributable to one of the joystick modes (at 110 Hz). From the *PSD*, however, it becomes clear that the acceleration sensors also pick up small contributions from other vibration modes:

- the other joystick mode (at 105 Hz; from this it becomes clear that, in practice, the assembly is not completely symmetrical);
- a mode around 140 Hz (torsion from the main plate; so, the main plate does deform, contrary to one of the assumptions made for the purpose of simplification in this article);
- modes around 280 Hz (the so-called pendulum modes, by which the lens moves more or less horizontally in the plane of suspension; see Figure 3).

Smart Disc concept

The so-called Smart Disc concept [1] enables collocated control. The Smart Disc is an active structural element for improving the dynamic behaviour of precision machinery and can be realised with the aid of piezoelectric material. This material can serve as an actuator (it expands under the influence of a voltage) but also as a sensor (when it is subjected to a force, an electric charge is the result).

Within the framework of the Smart Disc research project [1], two prototype active lens supports fitted with a piezoelectric position actuator and a piezoelectric force sensor were developed for the wafer scanner. The first prototype, the Smart Lens Support (SLS), was aimed at active damping of the joystick modes. In order to enable active damping of these modes by means of three identical SLSs, each SLS should locally display Smart Disc functionality in the vertical direction, i.e. have the ability to measure a local vertical force and produce a local vertical displacement.

SLS - mechanical design

The mechanical design of the Smart Lens Support [7] is based on the conventional lens support and has the same dimensions (100 x 20 x 60 mm^3). The two horizontal elastic hinges are copied, just as the foundation surfaces and the threaded holes for the bolts on the top and bottom sides.

The SLS is constructed from (see Figure 6):

- a flexure block;
- two actuator-sensor stacks, each consisting of an actuator (multi-layer, to be able to realise a reasonable expansion, even with a limited voltage) and a single-layer sensor;
- a preload bolt with two accompanying nuts.

Symmetry in the design should ensure purely vertical displacement when the actuators are controlled. In addition, the design contains an elastic preload element, which is necessary because piezoelectric material should not be subjected to tensile loads. As the adjustment of the mechanical preload is quite difficult, it was decided to place one preload bolt in the middle and two actuator-sensor stacks on the side of the SLS. Both actuators as well as both sensors are connected in electric parallel, so that, together, they ensure Smart Disc functionality in just one direction. An additional advantage of choosing two actuator-sensor stacks is the fact that the effective surface area of the actuator (and therefore the stiffness) is doubled.

SLS - actuator-sensor stack

As a basis for the actuator-sensor stack, a standard multilayer actuator with a surface area of 10 x 10 mm^2, a height of 18 mm and a maximum expansion of 15 μm are used. Because this is much more than the required expansion (eventually, 0.1 μm proved more than enough) and because there is only limited room in the lens support to build in the stacks, it was decided to cut one actuator into two smaller actuators (4 mm in height) and to mount a single-layer piezoelectric sensor (1 mm thick) onto them. Thin layers of passive ceramics were applied to both ends of the stack and between the actuator and the sensor as electric insulation. The resulting actuator-sensor stack (Figure 7) is 7.3 mm high.

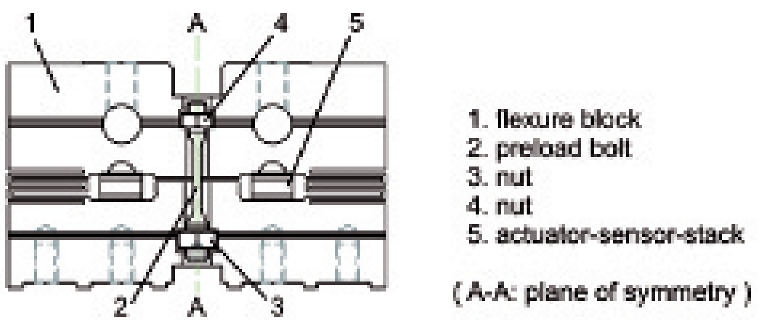

Figure 6. Smart Lens Support.

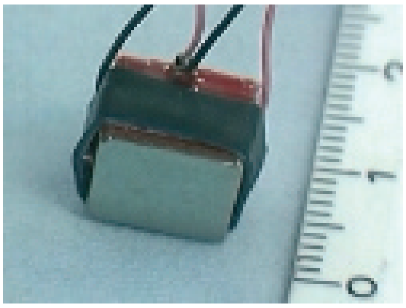

Figure 7. Bottom and front view of the actuator-sensor stack.

Another reason for keeping the height of the stacks so small is to limit the loss of the support's stiffness. Based on rough modelling, it was expected that the vertical stiffness of the SLS, determined mainly by the horizontal elastic hinges in series with the two parallel stacks, would amount to approximately half the stiffness of the conventional lens support. Although this is a drastic decline in stiffness, the design of the SLS (the stacks in particular) was not further optimised. The reason was the expectation that the given design would, in any case, enable Smart Disc experiments in the wafer scanner lens suspension.

SLS - flexure block

Figure 8 shows the front and two cross-section views of the SLS flexure block. In the middle of the block, two holes have been cut in which the actuator-sensor stacks can be placed. Between both holes, a horizontal incision was made and accordion springs were fitted on either side of the block. In addition, there is a vertical slot in the middle of the block in which the preload bolt and the nuts can be placed. The accordion springs ensure an elastic degree of freedom in (among others) the vertical direction between the top and bottom sides of the flexure block. The preload force they produce is insufficient under operational conditions, hence the need for the preload bolt.

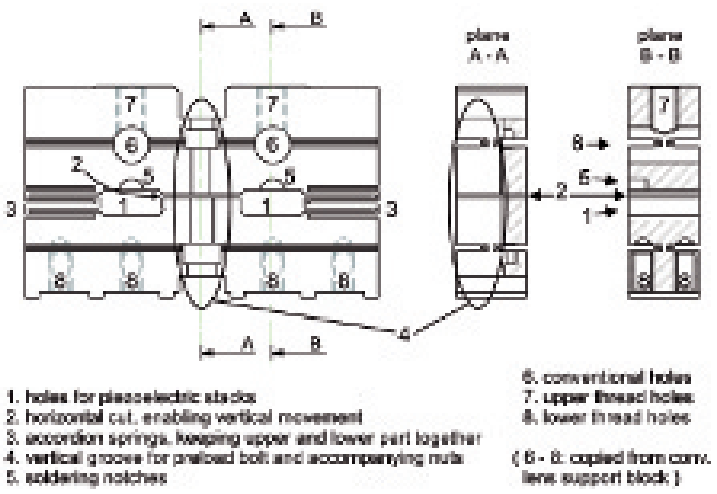

Figure 8. Front view and cross-section views of the SLS flexure block.

To fix the stacks in the flexure block, the preload force of the accordion springs alone would probably have been sufficient, but it was still decided to use glue on the top and bottom sides of the actuator-sensor stacks. The main purpose of this was to prevent damage to the piezoelectric material as a result of size discrepancies, roughness or unevenness; the disadvantage of glue is, once again, the decreased stiffness. For gluing, a specially designed gluing mould was used with which the correct final height of the SLS can be guaranteed. All tolerances are then absorbed into the two layers of glue (per stack) with an intended thickness of 2 x 0.05 mm.

Experiment with passive SLSs

Using the set-up as outlined in Figure 1, but now fitted with (passive) Smart Lens Supports, an experiment was carried out that was identical to the reference experiment with the conventional lens supports as described earlier. Figure 9 represents the results [6].

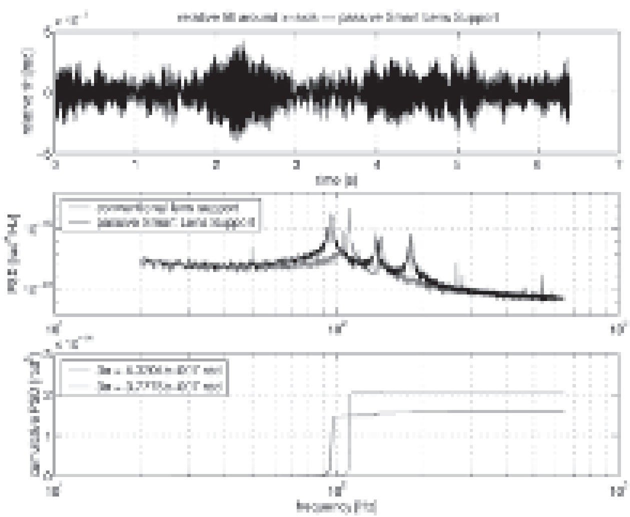

Figure 9. Results of the experiment with passive SLSs.

Conclusions from the *PSD* (central figure):

- The frequency of the joystick modes decreased from 110 to 96 Hz and from 105 to 92 Hz, respectively. This means that, as a consequence of the decreased vertical stiffness of the lens supports, the effective stiffness that plays a role in these modes decreased to $(92/105)^2 \approx 0.76$ of the original value.

- The frequency of the pendulum modes decreased from 274 to 184 Hz and from 266 to 179 Hz, respectively. This means that, as a result of the decreased tangential stiffness of the lens supports, the effective stiffness that plays a role in these modes decreased to $(179/266)^2 \approx 0.45$ of the original value.
- The frequency of the vibration mode around 140 Hz (torsion of the main plate) hardly decreased at all, which indicates that the stiffness of the lens supports in this mode hardly plays a role.

From the cumulative *PSD* (bottom figure) it can be deduced that, although the stiffness of the lens supports had decreased drastically, the average joystick rotation had not increased. In fact, in terms of the 3σ value, it turned out that the joystick rotation had actually decreased (from 0.43 μrad to 0.38 μrad). This reduction can be explained by the increased passive damping in the system, caused by a combination of hysteresis in the piezoelectric material, resistance in the actuator-sensor electronics (connected, but not powered) and the visco-elasticity of the glue. Further inspection of the measuring results has shown that the damping ratio of the joystick modes increased from 0.2% for the conventional lens support to 0.5% for the lens suspension with passive SLSs. Although the new value of the damping is still very small, its positive influence on the dynamic behaviour of the lens and the main plate is already apparent from the experiment. Therefore, actively increasing damping further seems eminently worthwhile.

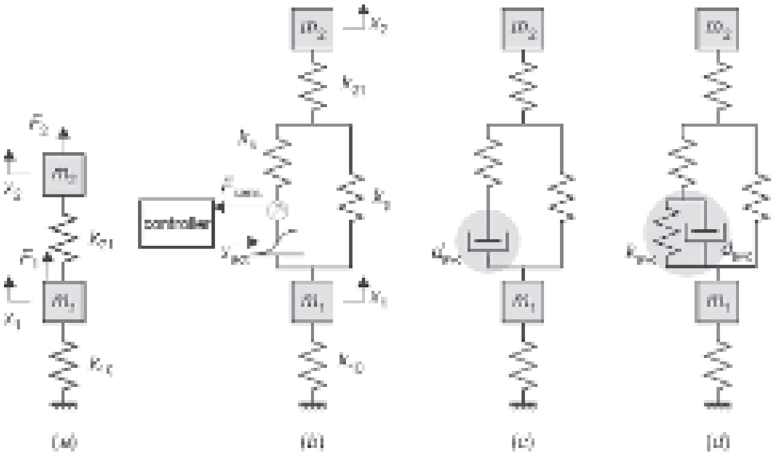

Figure 10. Illustration of the Smart Disc concept.
(a) Simple, undampened one-dimensional system.
(b) Smart Disc functionality added between both masses.
(c) Passive equivalent of a pure integrator in the controller.
(d) Passive equivalent of a leaking integrator in the controller.

Active damping: control engineering

The control strategy used to actively dampen by means of the SLS is based on the application of collocated control by which the behaviour of a passive element ('guaranteed' stable) can be actively realised (with the aid of actuators, sensors and amplifiers). To illustrate, Figure 10 shows the simple one-dimensional case in which a machine consists of two frame parts (m_1 and m_2) which are joined together with limited stiffness: $k_{21} < \infty$ (Figure 10a). Stiffness k_{10} represents an isolator.
A Smart Disc can be introduced into this configuration (Figure 10b). Passively, the actuator-sensor stack behaves mainly as an elastic element: k_s. Under the influence of an electric charge induced on the actuator, it will want to expand, which is indicated by the 'displacement source' x_{act}. The actual expansion, however, is dependent on a number of factors. Static displacement, for example, is dependent on the preload stiffness k_p. For reasons of efficiency as well as adjustability [1], it is advisable to minimize the preload stiffness.
The force in the actuator-sensor stack is measured (F_{sens}) and serves as an input signal for the controller. Together with the time derivative of the controlled position, this force constitutes a power conjugated variable pair: the product of the measured (compressive) force and the controlled velocity is equal to the power that flows from the mechanical system to the control system. If the sign of this product is positive at all times, it is certain that the control system extracts energy from the mechanical system. Thus, in an active way, the (passive) behaviour of a viscous damper is realised (Figure 10c). The controller simply has to prescribe a static linear relationship between the measured force and the velocity to be controlled:

$$v_{act}(t) = K\, F_{sens}(t),$$

which corresponds to a viscous damper with a value of

$$d_{avc} = F_{sens}/v_{act} = 1/K.$$

The control signal for the position actuator can be obtained by integrating $v_{act}(t)$:

$$x_{act}(t) = \int v_{act}(t)\mathrm{d}t = \int K\, F_{sens}(t)\mathrm{d}t = K \int F_{sens}(t)\mathrm{d}t$$

or, after Laplace transformation:

$$x_{act}(s) = \frac{K}{s} = F_{sens}(s).$$

This control strategy is referred to as Integral Force Feedback [5], [1].
In order to limit the control gain for low frequencies, a 'leaking integrator' is often used:

$$x_{act}(s) = \frac{K}{s+p} = F_{sens}(s),$$

with a static gain K/p. The passive equivalent of this controller is outlined in Figure 10d: parallel to the original damper $d_{avc} = 1/K$ appears an additional stiffness, represented by $k_{avc} = p/K$.
This control strategy is very robust and requires hardly any model knowledge. The only knowledge necessary is that the actuator and the sensor should be located at the same place in the system. For the performance of the control system it is, of course, important to tune the control parameters K and p correctly to the mechanical system. For this purpose, a set of tuning rules have been drawn up [1].
Crucial to implementing this method of active damping is a good balance between the values of the stiffness k_{avc} and the damper d_{avc} in Figure 10d. If k_{avc} is too large, the damper is hardly effective; if the value is too small, the stiffness of the whole system decreases too much [1].

Experiment with active SLSs

The control strategy was simultaneously applied to each of the three Smart Lens Supports in the wafer scanner lens suspension. After careful tuning, the same experiment was carried out as previously. The results are shown in Figure 11, [6], [1].
A comparison of the time domain signals with the reference experiments (the uppermost results in Figures 5, 9, and 11) shows that the joystick rotation has decreased significantly (note the scale along the vertical axis). The *PSD* shows that this is purely the result of increased damping of the joystick modes.
From the cumulative *PSD*, a measure can be distilled for the amplitude of the joystick rotation: the 3σ value has decreased from 0.43 μrad for the conventional lens supports, via 0.38 μrad for the passive SLS, to 0.10 μrad for the active SLSs. However, further inspection shows that only 0.06 μrad of this can be attributed to the joystick modes. When the whole frequency range is considered,

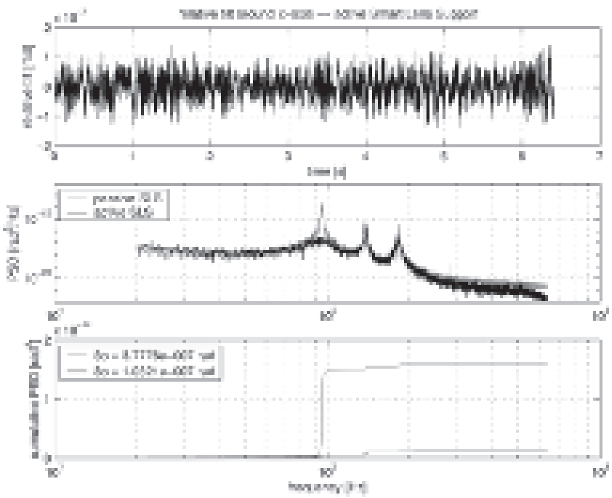

Figure 11. Results of the experiment with active SLSs.

there is a factor 4 improvement but, limited to the real rotation as a consequence of the joystick mode, there is a factor 7 improvement. A factor 80 even applies to the damping ratio of the joystick mode because this has increased from 0.2%, via 0.5%, to as much as 16%. In this way, lens vibrations can be reduced to less than 25% of the initial level.The pendulum modes, on the other hand, are hardly dampened with the SLS, simply because the actuator-sensor stacks are only active in a vertical direction.

Piezo Active Lens Mount

In order to be able to dampen the pendulum modes as well as the joystick modes, a second prototype lens support was developed, which is also active in the horizontal (or tangential) direction: the Piezo Active Lens Mount (PALM, [8], see Figure 12). The most notable changes in the SLS design for this purpose are:

- In the PALM, the actuator-sensor stacks are tilted 45°. By independently controlling and reading out the actuator-sensor stacks, two active degrees of freedom are created per PALM.
  - Controlling the actuators in phase results in a vertical displacement. The sum of the sensor signals is a measure for the vertical force on the PALM.
  - Control in anti-phase results in horizontal displacement of the upper part of the PALM in relation to the lower part. The difference between the sensor signals is a measure for the horizontal (shear) force on the PALM.

As a consequence of the piezos being tilted 45°, the PALM has an equally large actuation range in the horizontal and the vertical direction and the piezos deliver an equal contribution to PALM stiffness in both directions.
- To preserve the piezo material for possible shear stresses, additional flexure hinges with sufficient axial stiffness have been included in the flexure block around the sensor stacks.
- In the PALM design, the 'awkward' preload bolt has been omitted. The accordion springs are dimensioned in such a way that they can produce sufficient mechanical preload.
- As in the SLS, the piezos in the PALM are glued on with the aid of a special gluing mould. The glue is applied through special channels in the flexure block (see Figure 13).
- In view of possible use in other machine types, the height of the PALM has been changed from 60 mm to 85 mm. This does not benefit the stiffness of the lens suspension.

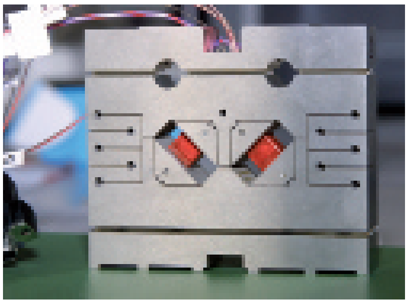

Figure 12. Piezo Active Lens Mount (photo: Job van Amerongen).

As with the SLS, it became clear that it is also quite possible to realise active damping with the PALM, albeit now for all six vibration modes of the lens with respect to the main plate – including the pendulum modes. The damping ratio for the various modes can even be enhanced to over 20%.

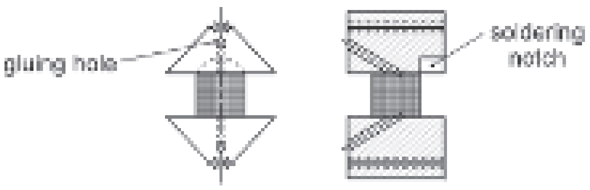

Figure 13. Detail of the PALM: glue channels. The soldering notch has been put in to enable soldering repairs to the piezo material electrodes.

Stiffness loss

Although the SLS as well as the PALM have proven to be eminently suitable for damping vibrations of the lens, both designs have a number of disadvantages. The main problem with both designs is the decreased stiffness of the lens suspension and, with that, the decreased natural frequencies. Table 1 shows the natural frequencies of the joystick and pendulum modes for the different lens supports. Based on this information, it was reconstructed how the effective vertical and horizontal stiffnesses of the SLS and the PALM relate to the stiffness of the conventional lens support (normalised at 100%).

Of course, some stiffness loss was factored in for both active lens supports, simply because two stacks of piezo material with a surface area of 10 x 10 mm^2 replace a 'slab of steel' with a surface area of 20 x 100 mm^2. With this in mind, the decrease in stiffness due to the SLS in the active, vertical direction was less than expected: from 100% to 76%. More alarming is the fact that the decrease in stiffness is so much larger in the non-active, horizontal direction of the SLS: from 100% to 45%.
It is the same with the PALM. Here, special attention was paid to sufficient axial stiffness in the design of the extra flexure hinges around the actuator-sensor stacks. With the tilting of the stacks, this had as a result that the extra stiffness loss in the horizontal direction remained within the limits: from 45% to 40%. In this case, the decrease in vertical stiffness is actually the most troubling: from 76% to 37%. This halving can be explained by the fact that whereas, in the SLS, all the axial piezo stiffness was available for the vertical direction, only half remains in the PALM, with the other half being employed in horizontal direction.
Why this has not led to an increase in total stiffness in horizontal direction can be explained by the fact that the horizontal stiffness in the SLS is made up by the shear stiffness of the piezos. As a result of the extra flexure hinges, meant to relieve the piezos of shearing, this shear stiffness – logically – no longer plays a role in the PALM.

For the SLS and the PALM, the conclusion is that the stiffness should have been dealt with more economically, especially in the non-active direction of the piezos.
As a result of the drastic stiffness loss, the PALM – in terms of the vibration levels on the lens and compared to the SLS – has hardly led to any improvement despite the increase in damping possibilities.

Table 1. Comparison of dominant vibration modes for different types of lens supports.

type of lens support	*joystick modes*			*pendulum modes*		
	frequency [Hz]	vertical stiffness	(active) damping	frequency [Hz]	horizontal stiffness	(active) damping
passive	107	100%	< 0.5%	270	100%	< 0.5%
SLS	94	76%	≈ 16%	181	45%	≈ 1.5%
PALM	65	37%	> 20%	170	40%	> 20%

Conclusion

The experiments described show that it is worthwhile to pay attention to realising sufficient damping in the design of precision machinery. Given the problems associated with designing 'reliable' passive damping mechanisms (based on phenomena that do not negatively influence accuracy), active damping seems to be a very suitable 'design principle' for this purpose. The relative ease with which active damping can be realised has been pointed out: an actuator and a sensor in one and the same, suitably chosen place in the system and a simple, robust control strategy. The experiments with the SLS and the PALM, built into a wafer scanner lens suspension, have shown that, in practice, vibrations can be reduced to less than 25% of the initial level.

On the basis of these experiences, piezoelectric material is pre-eminently suitable for the realisation of the actuator and sensor function in a machine frame. One disadvantage, however, is the inevitable loss of stiffness, rendering active damping at odds with the design principle of stiffness management. In the design of active structural elements, it is important, therefore, to minimise stiffness loss. It became clear from the stiffness analysis of the wafer scanner active lens supports that it is the stiffness in the *non-active* direction of the actuator and the sensor in particular that deserves special attention.

Authors' note

Jan Holterman and Theo J.A. de Vries are with imotec in Hengelo (Ov), the Netherlands. The Smart Disc project (1998-2004, University of Twente) was made possible in part by financial support from the Ministry of Economic Affairs within the framework of the Innovation Orientated Research Programme (IOP) Precision Technology.

References

[1] Holterman, J. (2002), *Vibration Control of High-precision Machines using Active Structural Elements*, thesis, University of Twente.

[2] Holterman, J. and T.J.A. de Vries (2002), "Actieve demping. Een nieuw constructie-principe?" (in Dutch), *Mikroniek*, no. 5.

[3] Holterman, J. and T.J.A. de Vries (2005), "Actieve demping haaks op optimale stijfheid? Optimale stijfheid haaks op actieve demping!" (in Dutch), *Mikroniek*, no. 4.

[4] Koster, M.P., (1998), *Constructieprincipes voor het nauwkeurig bewegen en positioneren* (in Dutch), 2nd impression, Twente University Press, Enschede, ISBN 9036511356.

[5] Preumont, A, (1997), *Vibration Control of Active Structures – An Introduction*, Kluwer Academic Publishers, Dordrecht, ISBN 0792343921.

[6] Jansen, B.S.H., (2000), *Smart Disc tuning and application*, thesis, University of Twente.

[7] Holterman, J. and B.G. Tacoma, (2001), *Smart Lens Support – mechanical design*, Report, Faculty of Electrical Engineering, University of Twente.

[8] Van den Elzen, S.A., (2001), *Design of a Smart Lens Support with Two Active Degrees of Freedom*, thesis, University of Twente.

Information

Tel. +31 (0)74 - 250 59 07
j.holterman@imotec.nl
www.imotec.nl
www.ce.utwente.nl/smartdisc